

Supporting Information for

Comparison of Two Field-Induced Er(III) Single Ion Magnets

Irina A. Kühne,^{*a,b} Liviu Ungur,^c Kane Esien,^{d,c} Anthony B. Carter,^{e,f} John D. Gordon,^b Cameron Pauly,^a Helge Müller-Bunz,^a Solveig Felton,^d Dominic Zerulla,^b and Grace G. Morgan^{*a}

Table of Contents

Table S1. Selected bond lengths of compound 1 – 4	2
Table S2. SHAPE analysis of compound 1 – 4	2
Figure S1. Magnetization curves for $[\text{ErL}_1\text{OAc}]\cdot\text{EtOH}\cdot\text{H}_2\text{O}$ (2) measured between 0 and 7 T.....	3
Figure S2. Magnetization curves for $[\text{ErL}_1(\text{CF}_3\text{CO}_2)]$ (4) measured between 0 and 7 T	3
Figure S3. In-phase (left) and out-of-phase susceptibility (right) of $[\text{ErL}_1\text{OAc}]\cdot\text{EtOH}\cdot\text{H}_2\text{O}$ (2)	3
Figure S4. In-phase (left) and out-of-phase susceptibility (right) of $[\text{ErL}_1(\text{CF}_3\text{CO}_2)]$ (4)	4
Figure S5. $\ln(\tau)$ versus $1/T$ for $[\text{ErL}_1\text{OAc}]\cdot\text{EtOH}\cdot\text{H}_2\text{O}$ (2) (left) and $[\text{ErL}_1(\text{CF}_3\text{CO}_2)]$ (4) (right).....	4
Figure S6. Temperature-dependence of the in-phase (left) and out-of-phase susceptibility (right) of $[\text{ErL}_1\text{OAc}]\cdot\text{EtOH}\cdot\text{H}_2\text{O}$ (2) at 500 Oe at varying frequencies between 1 Hz and 1500 Hz.....	5
Figure S7. Cole-Cole plot between 1.8 and 4.0 K for $[\text{ErL}_1\text{OAc}]\cdot\text{EtOH}\cdot\text{H}_2\text{O}$ (2) (left) and $[\text{ErL}_1(\text{CF}_3\text{CO}_2)]$ (4) (right) both measured at 500 Oe.	5
Figure S8. Frequency-dependence of the in-phase (left) and out-of-phase susceptibility (right) at 1500 Oe of $[\text{ErL}_1(\text{CF}_3\text{CO}_2)]$ (4) in a temperature range between 1.8–4.0 K	6
Figure S9. Cole-Cole plot between 1.8 and 3.0 K for $[\text{ErL}_1(\text{CF}_3\text{CO}_2)]$ (4) (left) and a zoom in for highlighting the second process (right), measured at 1500 Oe.....	6
Table S3. Resulting parameters of τ and α obtained with CC-Fit of $[\text{ErL}_1\text{OAc}]\cdot\text{EtOH}\cdot\text{H}_2\text{O}$ (2) at 500 Oe.6	6
Table S4. Resulting parameters of τ and α obtained with CC-Fit of $[\text{ErL}_1(\text{CF}_3\text{CO}_2)]$ (4) at 500 Oe.	7
Table S5. Resulting parameters of τ and α obtained with CC-Fit of $[\text{ErL}_1(\text{CF}_3\text{CO}_2)]$ (4) at 1500 Oe.	7
Figure S10. Solid state diffuse spectral reflectance spectra of Gd containing complexes 1 and 3	8
Figure S11. IR spectrum of $[\text{Gd}(\text{L}_1)(\text{OAc})]\cdot\text{EtOH}\cdot\text{H}_2\text{O}$ (1).	9
Figure S12. IR spectrum of $[\text{Er}(\text{L}_1)(\text{OAc})]\cdot\text{EtOH}\cdot\text{H}_2\text{O}$ (2).....	9
Figure S13. Fingerprint-region of the IR spectrum of $[\text{Er}(\text{L}_1)(\text{OAc})]\cdot\text{EtOH}\cdot\text{H}_2\text{O}$ (2).	10
Figure S14. IR spectrum of $[\text{Gd}(\text{L}_1)(\text{CF}_3\text{CO}_2)]$ (3).	10
Figure S15. Fingerprint-region of the IR spectrum of $[\text{Gd}(\text{L}_1)(\text{CF}_3\text{CO}_2)]$ (3).	11
Figure S16. IR spectrum of $[\text{Er}(\text{L}_1)(\text{CF}_3\text{CO}_2)]$ (4).	11
Figure S17. Fingerprint-region of the IR spectrum of $[\text{Er}(\text{L}_1)(\text{CF}_3\text{CO}_2)]$ (4).....	12
Figure S18. Solid state Raman spectra of both Er ^{III} containing complexes 2 (blue) and 4 (green) using a 532 nm laser excitation.	12
Table S6. Selected crystallographic data for 1–4	12

Table S1. Selected bond lengths of compound **1 – 4**.

Compound	[GdL ₁ (OAc)]·H ₂ O ·EtOH (1)	[ErL ₁ (OAc)]·H ₂ O ·EtOH (2)	[GdL ₁ (CF ₃ CO ₂)] (3)	[ErL ₁ (CF ₃ CO ₂)] (4)
sample code	IK153 – mor1197	IK273 – mor1276	IK218 – mor1214	IK291 – mor1301
Ln-O(1)	2.260(2)	2.210(5)	2.230(3)	2.1721(17)
Ln-O(4)	2.266(2)	2.210(5)	2.215(2)	2.1757(18)
Ln-O(5)	2.335(2)	2.286(5)	2.447(3)	2.3858(19)
Ln-N(1)	2.539(3)	2.494(6)	2.567(3)	2.522(2)
Ln-N(2)	2.603(2)	2.567(6)	2.567(5) (A); 2.615(19) (B)	2.525(4) (A); 2.554(15) (B)
Ln-N(3)	2.616(3)	2.569(7)	2.610(3)	2.562(2)
Ln-N(4)	2.567(3)	2.531(6)	2.598(3)	2.554(2)
Ln-N(5)	2.556(3)	2.517(6)	2.520(3)	2.483(2)

Table S2. SHAPE analysis of compound **1 – 4**.

OP-8: Octagon; HPY-8: Heptagonal pyramid; HBPY-8: Hexagonal bipyramid; CU-8: Cube; SAPR-8: Square antiprism; TDD-8: Triangular dodecahedron; JGBF-8: Johnson gyrobifastigium; JETBPY-8: Johnson elongated triangular bipyramid; JBTPR-8: Biaugmented trigonal prism; BTPR-8: Biaugmented trigonal prism; JSD-8: Snub diphenoid; TT-8: Triakis tetrahedron; ETBPY-8: Elongated trigonal bipyramid.

	[GdL ₁ (OAc)]·H ₂ O ·EtOH (1)	[ErL ₁ (OAc)]·H ₂ O ·EtOH (2)	[GdL ₁ (CF ₃ CO ₂)] (3)	[ErL ₁ (CF ₃ CO ₂)] (4)	
sample code	IK153 – mor1197	IK273 – mor1276	IK218 - mor1214 site A site B	IK291 – mor1301 site A site B	
OP-8	31.536	31.105	31.121	31.606	31.232
HPY-8	22.528	22.470	22.214	22.949	23.087
HBPY-8	12.354	12.901	12.776	13.141	13.513
CU-8	9.448	9.966	10.588	12.533	12.417
SAPR-8	2.369	2.215	2.821	3.460	3.114
TDD-8	2.219	1.987	1.715	1.739	1.510
JGBF-8	10.001	10.222	9.928	8.549	8.940
JETBPY-8	26.610	27.066	26.789	27.085	27.086
JBTPR-8	2.264	2.047	2.734	2.972	2.733
BTPR-8	1.887	1.740	2.402	2.663	2.439
JSD-8	2.659	2.419	2.283	2.257	2.029
TT-8	10.166	10.658	11.197	13.005	12.870
ETBPY-8	23.201	23.504	24.031	23.525	23.934

In case of complex **3** and **4**, one Nitrogen atom of the ligand backbone shows a disorder in the crystal structure, leading to N2A and N2B in the structure, which were treated separately, leading to site A and site B of the same molecule.

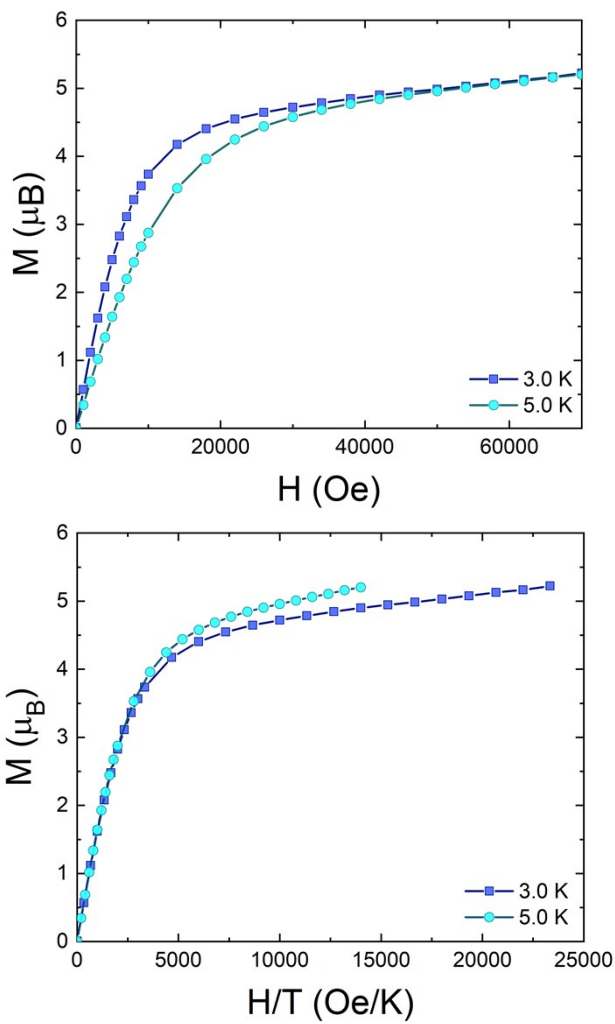


Figure S1. Magnetization curves for $[\text{ErL}_1\text{OAc}]\cdot\text{EtOH}\cdot\text{H}_2\text{O}$ (**2**) measured between 0 and 7 T at different temperatures (left) and reduced magnetization (right).

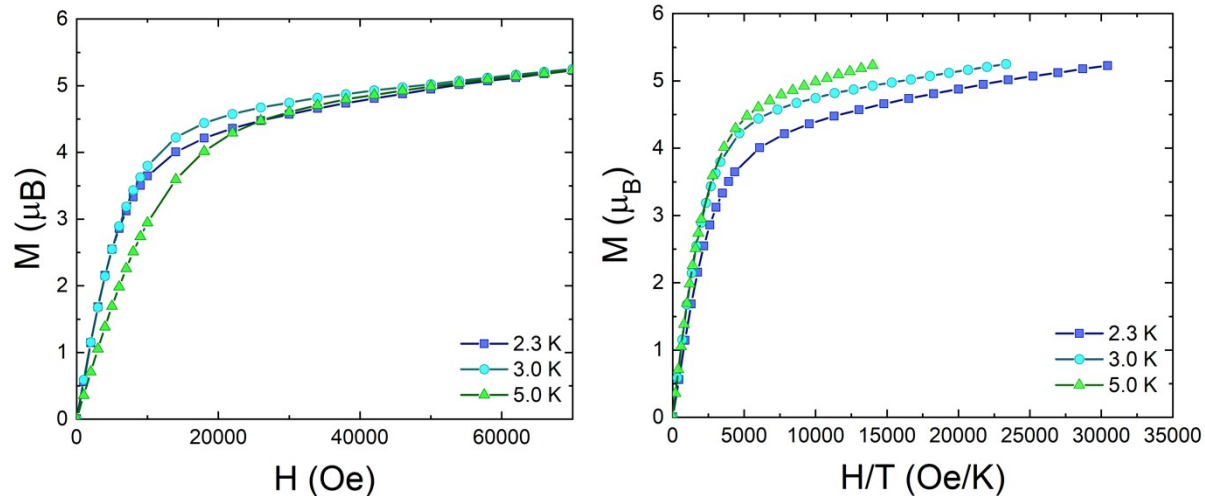


Figure S2. Magnetization curves for $[\text{ErL}_1(\text{CF}_3\text{CO}_2)]$ (**4**) measured between 0 and 7 T at different temperatures (left) and reduced magnetization (right).

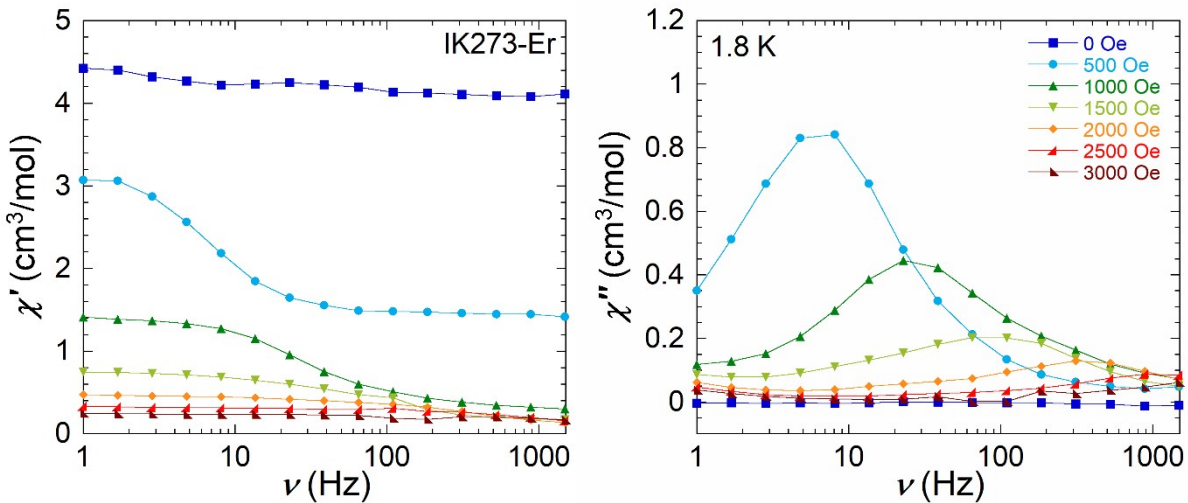


Figure S3. In-phase (left) and out-of-phase susceptibility (right) of $[\text{ErL}_1\text{OAc}]\cdot\text{EtOH}\cdot\text{H}_2\text{O}$ (2) at varying field between 0 Oe and 3000 Oe.

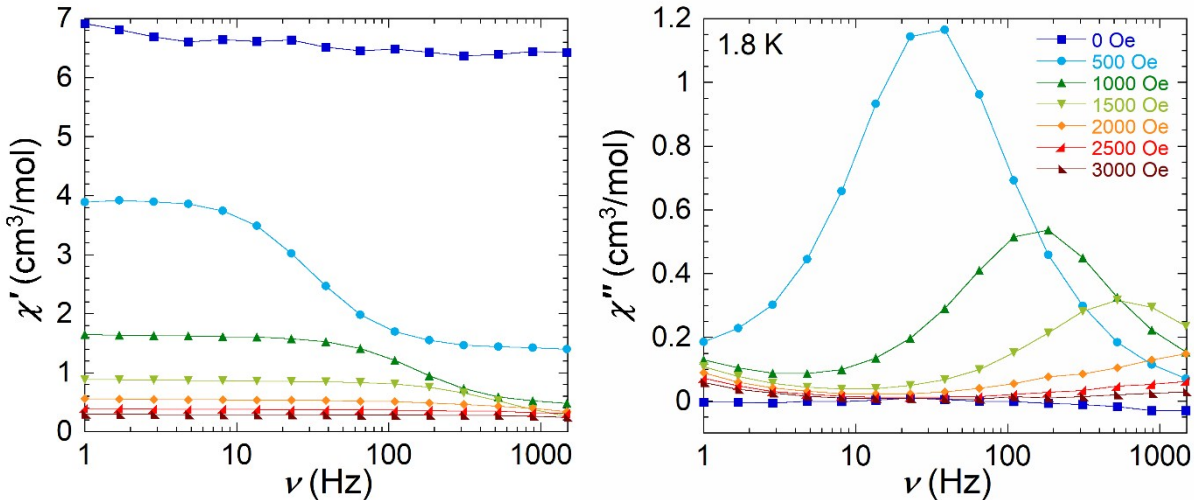


Figure S4. In-phase (left) and out-of-phase susceptibility (right) of $[\text{ErL}_1(\text{CF}_3\text{CO}_2)]$ (4) at varying field between 0 Oe and 3000 Oe.

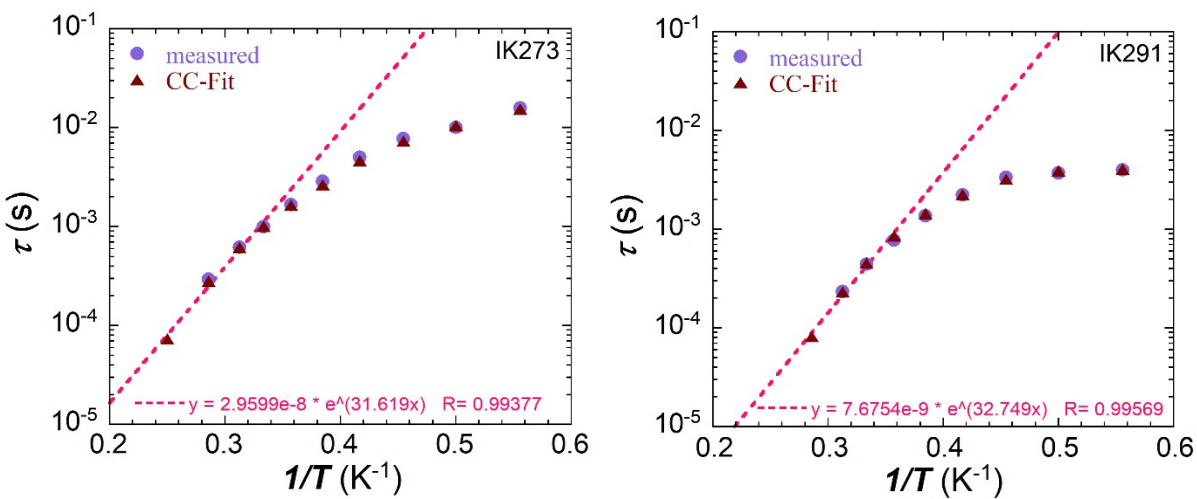


Figure S5. $\ln(\tau)$ versus $1/T$ for $[\text{ErL}_1\text{OAc}]\cdot\text{EtOH}\cdot\text{H}_2\text{O}$ (2) (left) and $[\text{ErL}_1(\text{CF}_3\text{CO}_2)]$ (4) (right) with the τ -values obtained by the out-of-phase maxima (purple circles) or the Cole-Cole fit (red triangles) and the Arrhenius fit as dashed pink line.

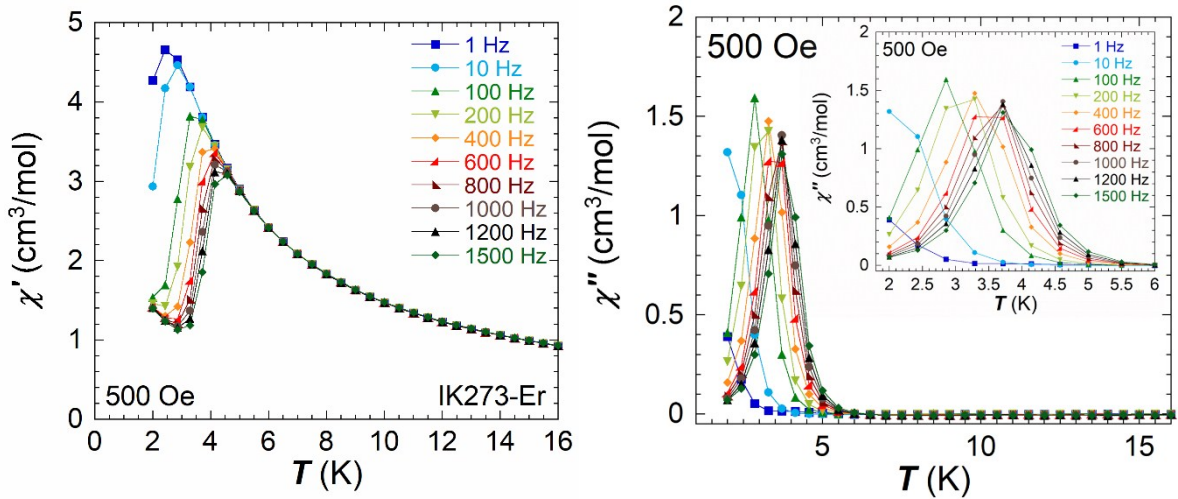


Figure S6. Temperature-dependence of the in-phase (left) and out-of-phase susceptibility (right) of $[\text{ErL}_1\text{OAc}]\cdot\text{EtOH}\cdot\text{H}_2\text{O}$ (**2**) at 500 Oe at varying frequencies between 1 Hz and 1500 Hz.

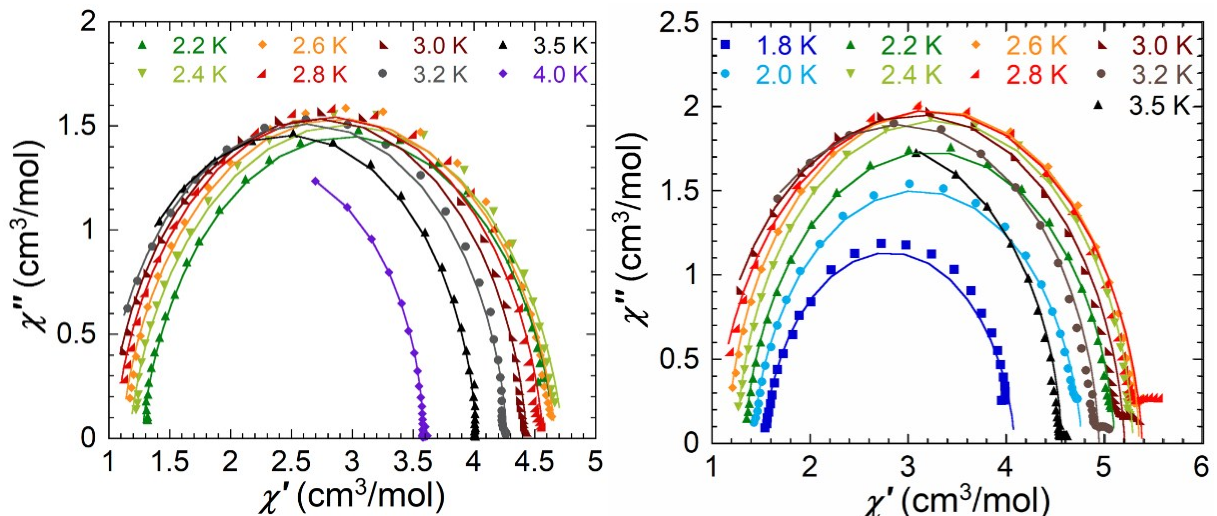


Figure S7. Cole-Cole plot between 1.8 and 4.0 K for $[\text{ErL}_1\text{OAc}]\cdot\text{EtOH}\cdot\text{H}_2\text{O}$ (**2**) (left) and $[\text{ErL}_1(\text{CF}_3\text{CO}_2)]$ (**4**) (right) both measured at 500 Oe.
Solid lines are fits of the experimental data using CC-Fit which uses a generalized Debye model.

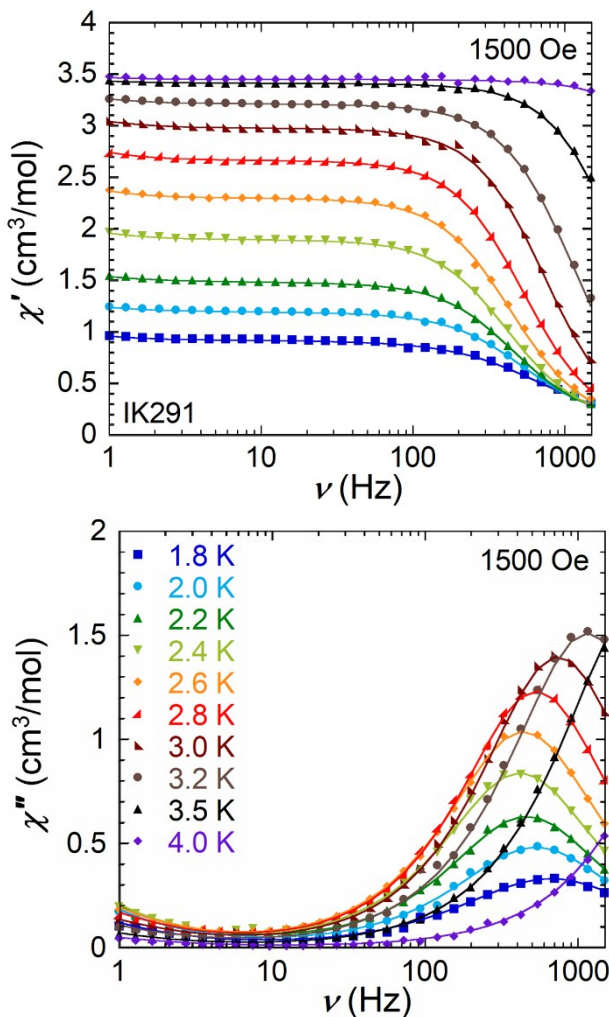


Figure S8. Frequency-dependence of the in-phase (left) and out-of-phase susceptibility (right) at 1500 Oe of $[\text{ErL}_1(\text{CF}_3\text{CO}_2)]$ (**4**) in a temperature range between 1.8-4.0 K (solid line represents the best fit obtained using CC-Fit which uses a generalized Debye model).

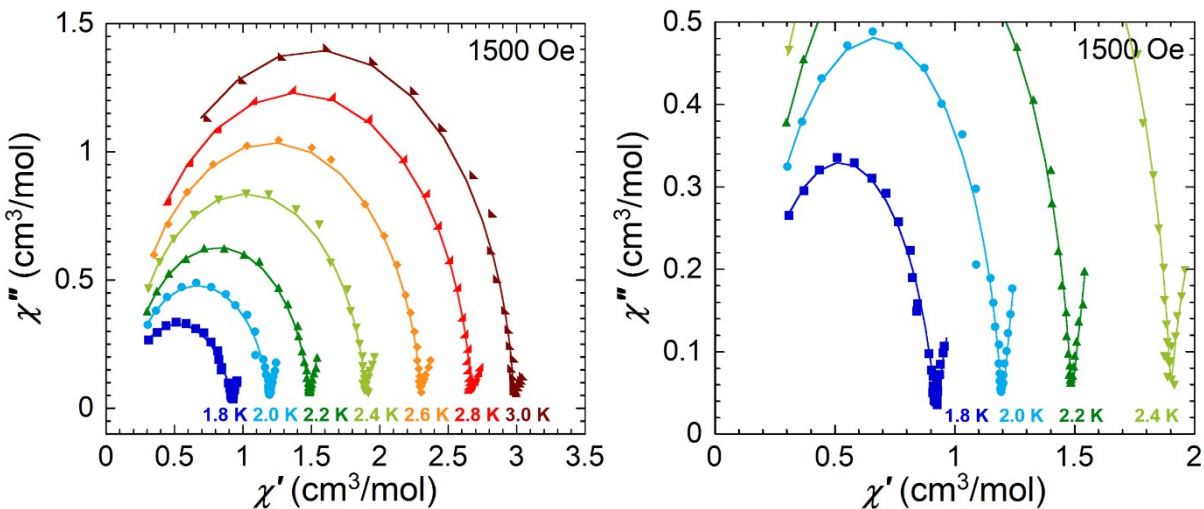


Figure S9. Cole-Cole plot between 1.8 and 3.0 K for $[\text{ErL}_1(\text{CF}_3\text{CO}_2)]$ (**4**) (left) and a zoom in for highlighting the second process (right), measured at 1500 Oe. Solid lines are fits of the experimental data using CC-Fit which uses a generalized Debye model.

Table S3. Resulting parameters of τ and α obtained with CC-Fit of $[\text{ErL}_1\text{OAc}]\cdot\text{EtOH}\cdot\text{H}_2\text{O}$ (2) at 500 Oe.

```
#####
##### CC-FIT #####
#####
##### (C) 2014 #####
##### NICHOLAS F CHILTON #####
##### nfchilton@gmail.com #####
#####
```

Number of relaxation processes: 1

Number of temperatures: 10

Number of frequencies: 30

T(K)	ChiS	ChiT	Tau	Alpha	Residual
1.8	0.138537E+01	0.407440E+01	0.153934E-01	0.156145E+00	0.597438E+00
2.0	0.132008E+01	0.455639E+01	0.105085E-01	0.120006E+00	0.161903E+00
2.2	0.127001E+01	0.466585E+01	0.732078E-02	0.100385E+00	0.988388E-01
2.4	0.116658E+01	0.473288E+01	0.462661E-02	0.107296E+00	0.135827E+00
2.6	0.110091E+01	0.467104E+01	0.264654E-02	0.955942E-01	0.106966E+00
2.8	0.104253E+01	0.457059E+01	0.163797E-02	0.848873E-01	0.934458E-01
3.0	0.995977E+00	0.443510E+01	0.101304E-02	0.727326E-01	0.558754E-01
3.2	0.956147E+00	0.427235E+01	0.617049E-03	0.595186E-01	0.320502E-01
3.5	0.903400E+00	0.402144E+01	0.281435E-03	0.435620E-01	0.121025E-01
4.0	0.872766E+00	0.358642E+01	0.734646E-04	0.175601E-01	0.295716E-02

Table S4. Resulting parameters of τ and α obtained with CC-Fit of $[\text{ErL}_1(\text{CF}_3\text{CO}_2)]$ (4) at 500 Oe.

```
#####
##### CC-FIT #####
#####
##### (C) 2014 #####
##### NICHOLAS F CHILTON #####
##### nfchilton@gmail.com #####
#####
```

Number of relaxation processes: 1

Number of temperatures: 9

Number of frequencies: 30

T(K)	ChiS	ChiT	Tau	Alpha	Residual
1.8	0.152352E+01	0.408185E+01	0.405303E-02	0.780620E-01	0.178985E+00
2.0	0.141577E+01	0.476605E+01	0.389407E-02	0.711197E-01	0.892546E-01
2.2	0.133404E+01	0.510102E+01	0.322102E-02	0.543167E-01	0.501062E-01
2.4	0.125393E+01	0.528488E+01	0.224146E-02	0.324655E-01	0.280252E-01
2.6	0.115745E+01	0.534986E+01	0.143719E-02	0.373360E-01	0.188724E+00
2.8	0.102586E+01	0.538030E+01	0.849892E-03	0.626908E-01	0.444317E+00
3.0	0.946529E+00	0.520089E+01	0.454991E-03	0.559672E-01	0.230059E+00
3.2	0.878609E+00	0.494047E+01	0.232787E-03	0.458088E-01	0.107465E+00

3.5 0.780403E+00 0.456055E+01 0.821507E-04 0.378735E-01 0.352503E-01

Table S5. Resulting parameters of τ and α obtained with CC-Fit of $[\text{ErL}_1(\text{CF}_3\text{CO}_2)]$ (**4**) at 1500 Oe.

```
#####
##### CC-FIT #####
#####
##### (C) 2014 #####
##### NICHOLAS F CHILTON #####
##### nfchilton@gmail.com #####
#####
```

Number of relaxation processes: 2

Number of temperatures: 10

Number of frequencies: 30

ChiS(total)	dChi1	Tau1	Alpha1	dChi2	Tau2	Alpha2	Residual
0.121552E+00	0.802396E+00	0.240242E-03	0.124321E+00	0.506201E+00	0.691765E+00	0.685631E-01	0.309490E-02
0.145508E+00	0.104865E+01	0.301518E-03	0.559929E-01	0.308152E+01	0.410188E+01	0.136626E+00	0.327212E-02
0.153220E+00	0.133001E+01	0.346978E-03	0.361235E-01	0.313065E+01	0.386629E+01	0.149002E+00	0.320113E-02
0.143786E+00	0.175388E+01	0.380674E-03	0.295963E-01	0.100455E+01	0.821577E+00	0.727833E-01	0.890329E-02
0.123744E+00	0.217740E+01	0.361923E-03	0.314682E-01	0.720291E+00	0.587357E+00	0.632583E-01	0.115481E-01
0.115085E+00	0.255273E+01	0.299180E-03	0.232331E-01	0.505615E+00	0.431956E+00	0.621315E-01	0.659930E-02
0.823903E-01	0.289695E+01	0.214880E-03	0.226389E-01	0.458705E+00	0.514632E+00	0.103989E+00	0.185449E-01
0.212276E-15	0.321656E+01	0.136935E-03	0.401018E-01	0.368568E+00	0.531902E+00	0.856994E-01	0.276395E-01
0.352405E-15	0.341471E+01	0.644790E-04	0.285304E-01	0.416326E+00	0.111599E+01	0.105482E+00	0.827524E-02
0.921607E-15	0.345200E+01	0.165057E-04	0.288412E-01	0.113401E+00	0.318362E+00	0.489844E-12	0.463239E-02

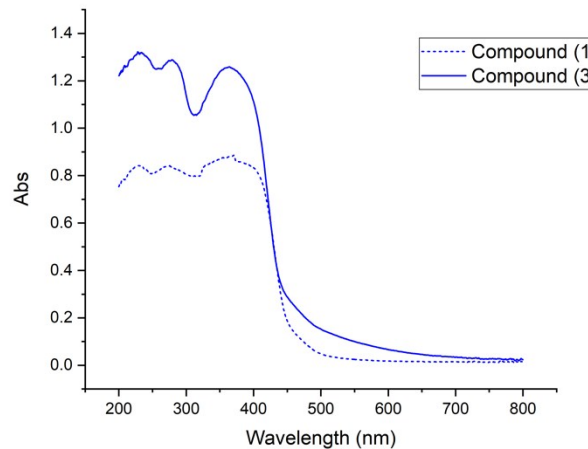


Figure S10. Solid state diffuse spectral reflectance spectra of Gd containing complexes **1** and **3**.

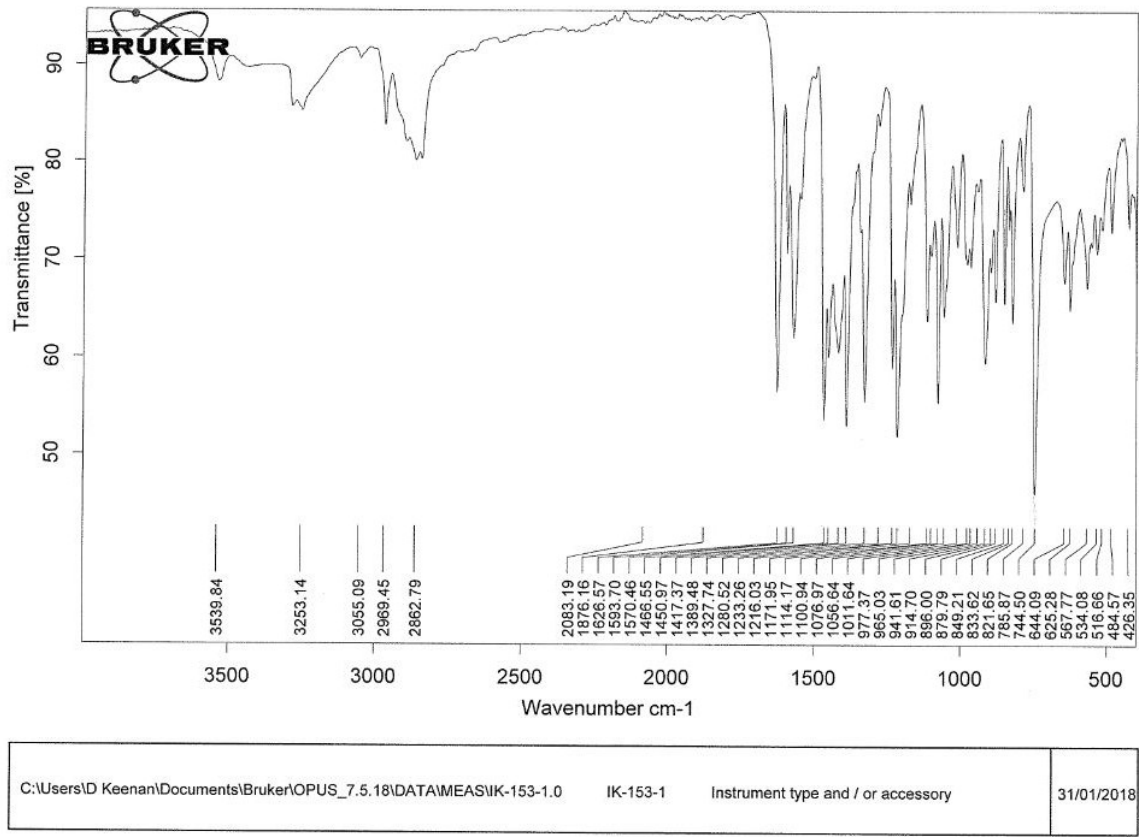


Figure S11. IR spectrum of $[\text{Gd}(\text{L}_1)(\text{OAc})]\cdot\text{EtOH}\cdot\text{H}_2\text{O}$ (**1**).

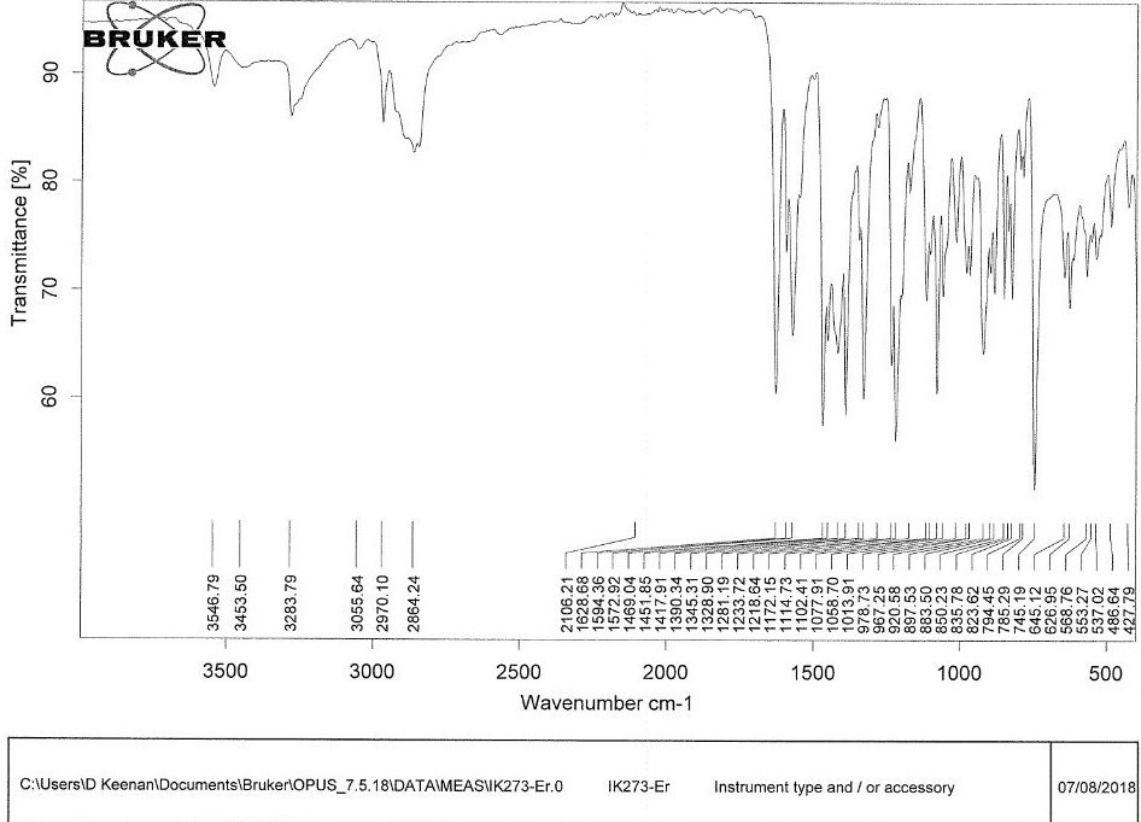


Figure S12. IR spectrum of $[\text{Er}(\text{L}_1)(\text{OAc})]\cdot\text{EtOH}\cdot\text{H}_2\text{O}$ (**2**).

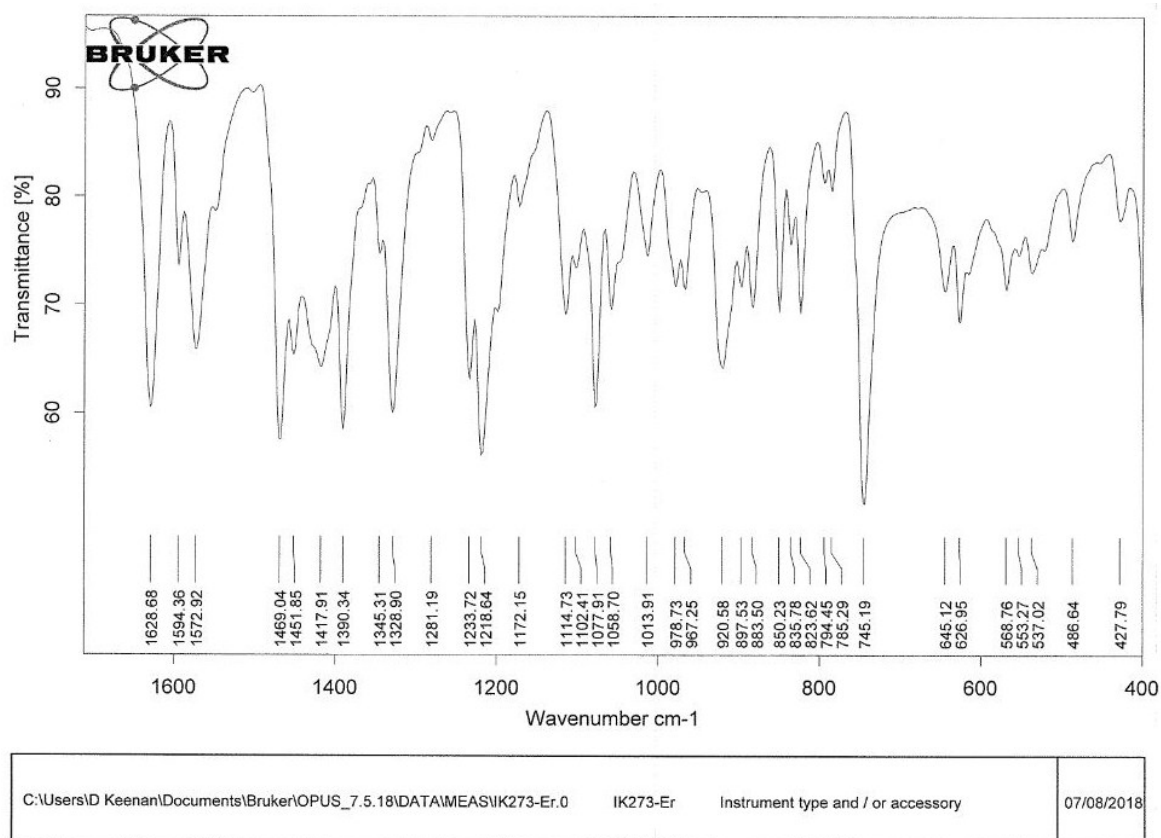


Figure S13. Fingerprint-region of the IR spectrum of $[\text{Er}(\text{L}_1)(\text{OAc})]\cdot\text{EtOH}\cdot\text{H}_2\text{O}$ (2).

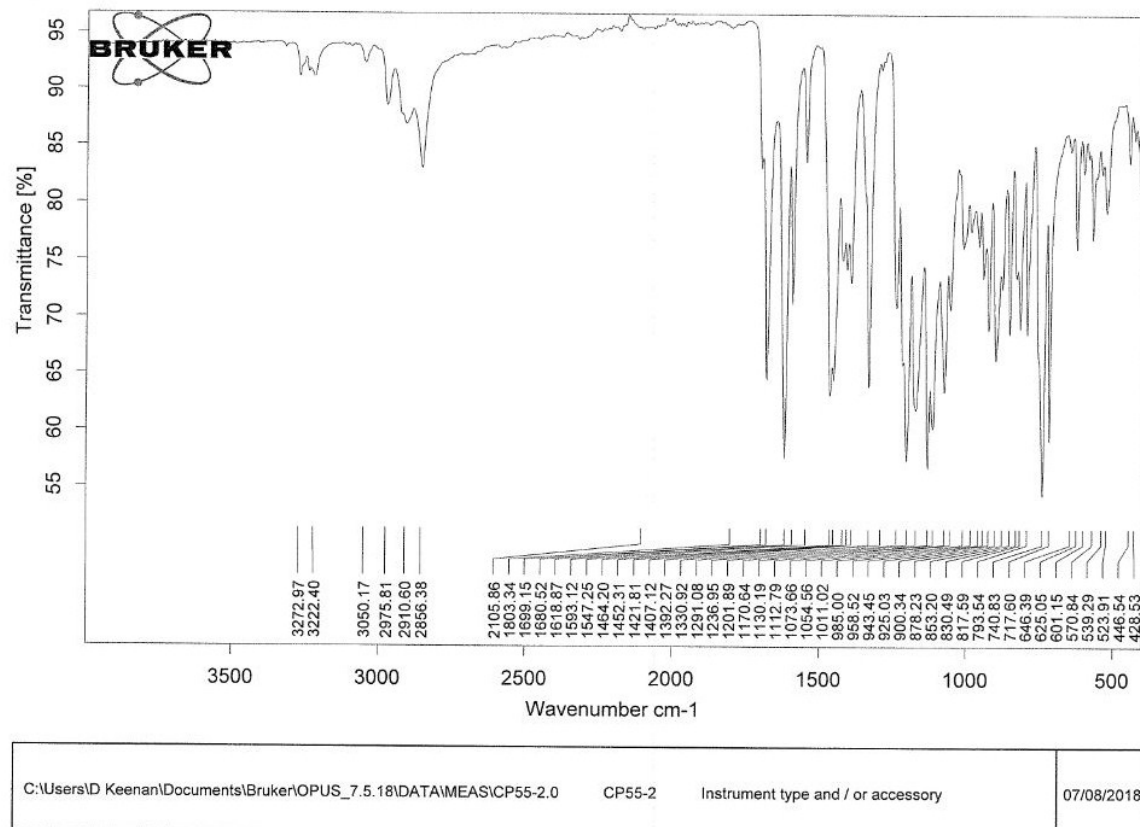


Figure S14. IR spectrum of $[\text{Gd}(\text{L}_1)(\text{CF}_3\text{CO}_2)]$ (3).

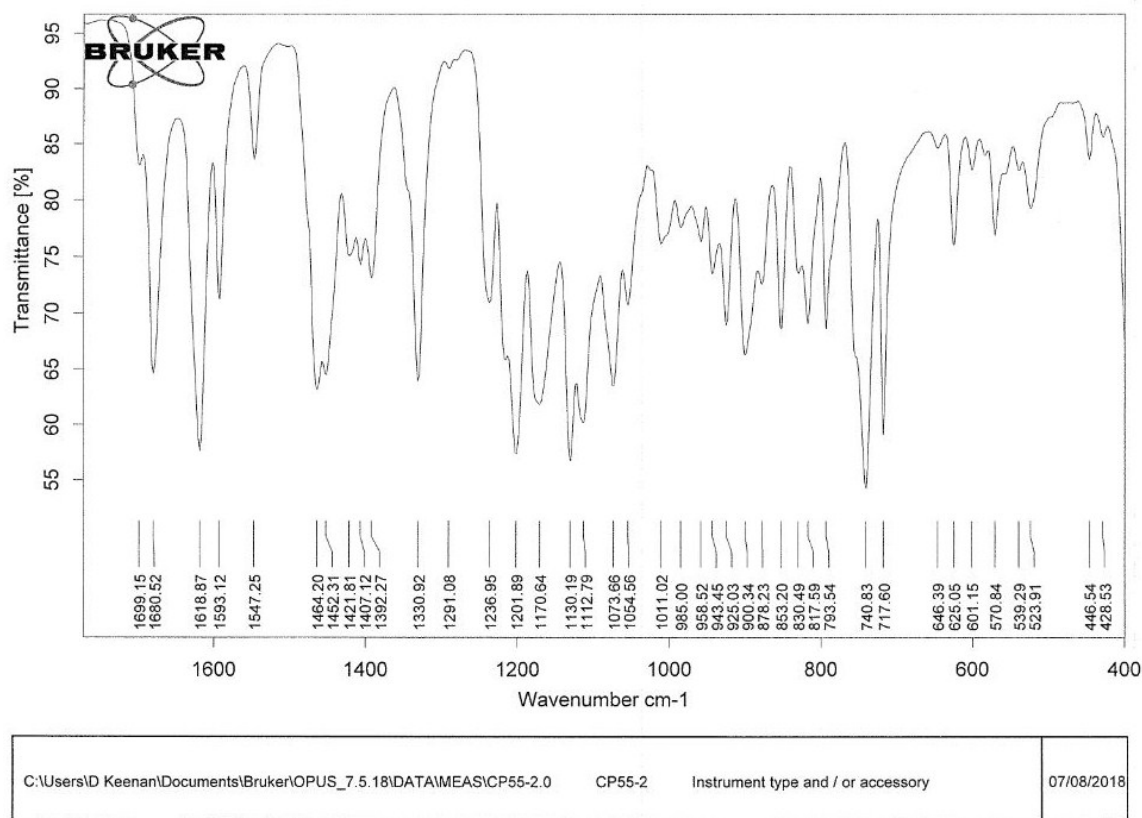


Figure S15. Fingerprint-region of the IR spectrum of $[Gd(L_1)(CF_3CO_2)]$ (3).

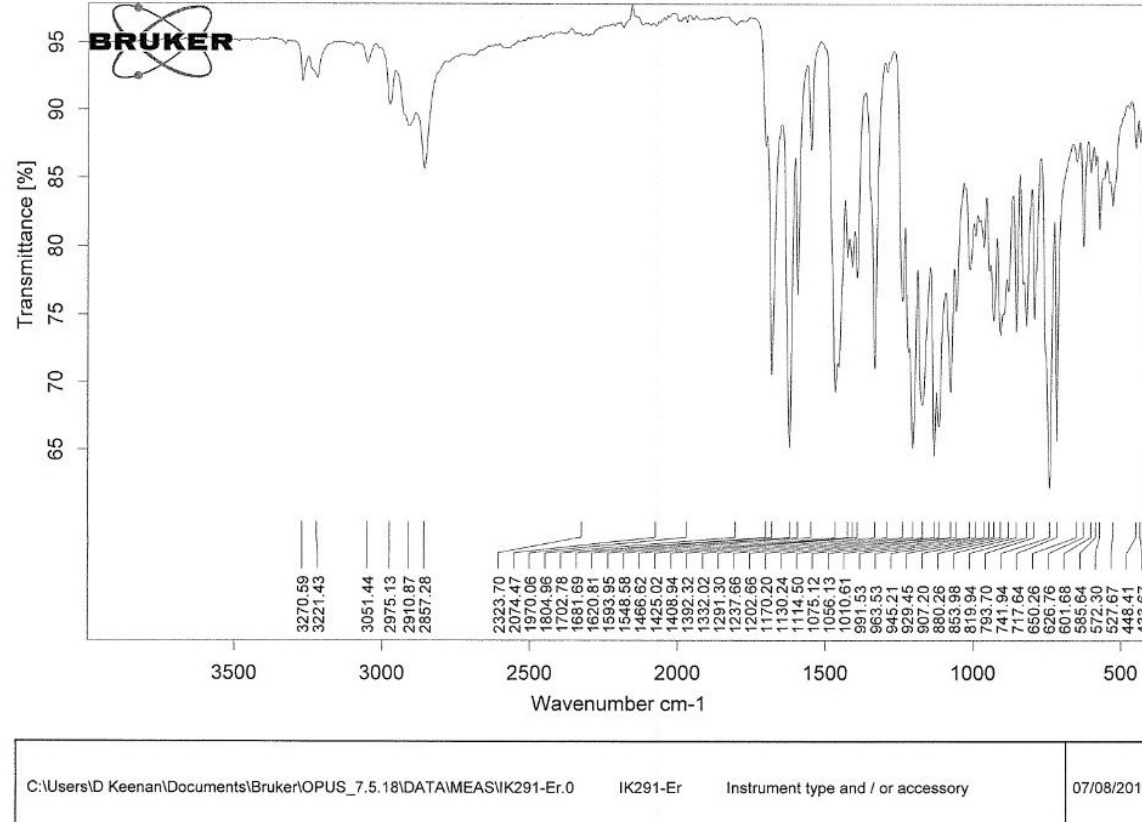


Figure S16. IR spectrum of $[Er(L_1)(CF_3CO_2)]$ (4).

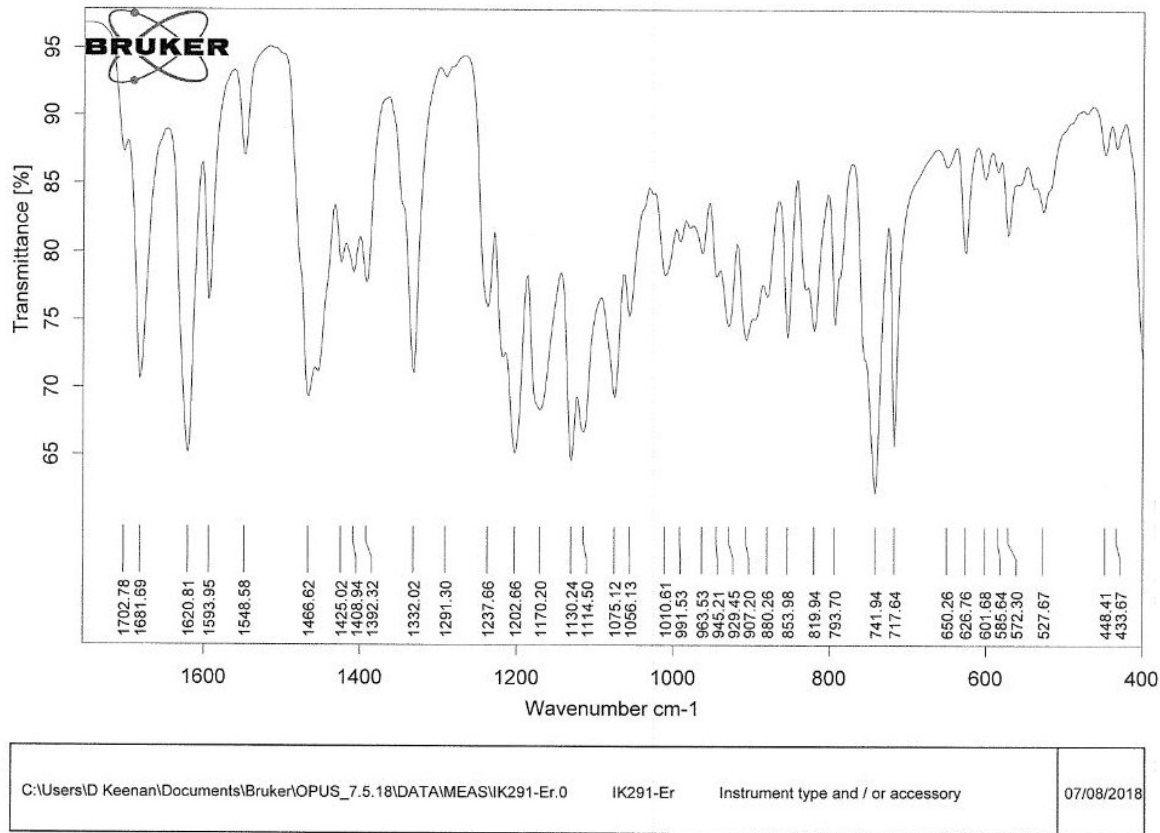


Figure S17. Fingerprint-region of the IR spectrum of $[\text{Er}(\text{L}_1)(\text{CF}_3\text{CO}_2)]$ (**4**).

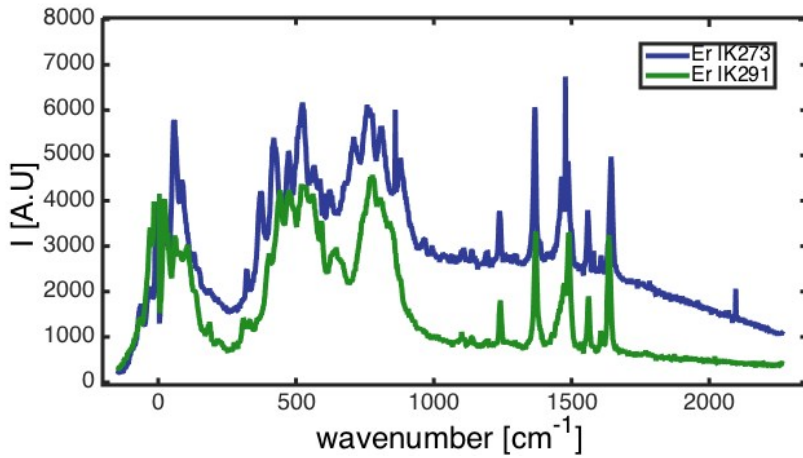


Figure S18. Solid state Raman spectra of both Er^{III} containing complexes **2** (blue) and **4** (green) using a 532 nm laser excitation.

Table S6. Selected crystallographic data for **1-4**.

Compound	$[\text{GdL}_1(\text{OAc})]\cdot\text{EtOH}\cdot\text{H}_2\text{O}$ 1	$[\text{ErL}_1(\text{OAc})]\cdot\text{EtOH}\cdot\text{H}_2\text{O}$ 2	$[\text{GdL}_1(\text{CF}_3\text{CO}_2)]$ 3	$[\text{ErL}_1(\text{CF}_3\text{CO}_2)]$ 4
sample code	IK153 – mor1197	IK273 – mor1276	IK218 – mor1214	IK291 – mor1301
Empirical formula	$\text{C}_{30}\text{H}_{48}\text{N}_5\text{O}_8\text{Gd}$	$\text{C}_{30}\text{H}_{48}\text{N}_5\text{O}_8\text{Er}$	$\text{C}_{28}\text{H}_{37}\text{N}_5\text{O}_6\text{F}_3\text{Gd}$	$\text{C}_{28}\text{H}_{37}\text{N}_5\text{O}_6\text{F}_3\text{Er}$
Formula weight	763.98	773.99	753.87	763.88
Crystal system	orthorhombic	orthorhombic	monoclinic	monoclinic

Space group	<i>P2₁2₁2₁</i>	<i>P2₁2₁2₁</i>	<i>P2₁/c</i>	<i>P2₁/c</i>
Crystal size (nm)	0.217 x 0.217 x 0.197	0.362 x 0.251 x 0.187	0.239 x 0.114 x 0.037	0.310 x 0.222 x 0.069
<i>a</i> (Å)	10.5109(2)	10.6073(3)	12.7436(2)	12.9038(2)
<i>b</i> (Å)	15.1977(2)	15.3338(4)	16.4518(3)	16.5260(2)
<i>c</i> (Å)	20.4077(3)	20.4350(5)	14.9252(2)	14.9360(2)
α (°)	90	90	90	90
β (°)	90	90	105.429(2)	106.172(2)
γ (°)	90	90	90	90
V (Å ³)	3259.96(9)	3323.76(15)	3016.37(9)	3059.04(8)
Z	4	4	4	4
d _{calc} (g cm ⁻³)	1.557	1.547	1.660	1.659
<i>T</i> (K)	100(2)	293(2)	100(2)	190(2)
μ (mm ⁻¹)	2.090	2.579	14.816	2.810
F(000)	1564	1580	1516	1532
Limiting indices	$h = \pm 15, k = \pm 23, l = \pm 31$	$h = \pm 13, k = \pm 19, l = \pm 25$	$h = \pm 16, k = \pm 20, l = \pm 18$	$h = \pm 18, k = \pm 23, l = \pm 21$
Reflections collected / unique	75174 / 11556	20346 / 7128	17024 / 6293	49974 / 8946
R(int)	0.0520	0.0493	0.0316	0.0301
Completeness to Θ (%)	99.7	99.6	100.0	99.8
Data / restraints / parameters	11556 / 0 / 405	7128 / 0 / 405	6293 / 0 / 399	8946 / 0 / 425
GooF on F ²	1.052	1.041	1.060	1.073
Final R indices [I > 2σ(I)] ^a	R ₁ = 0.0266, wR ₂ = 0.0440	R ₁ = 0.0379, wR ₂ = 0.0851	R ₁ = 0.0359, wR ₂ = 0.0892	R ₁ = 0.0263, wR ₂ = 0.0541
R indices (all data)	R ₁ = 0.0335, wR ₂ = 0.0466	R ₁ = 0.0438, wR ₂ = 0.0909	R ₁ = 0.0404, wR ₂ = 0.0925	R ₁ = 0.0337, wR ₂ = 0.0574
Largest diff. peak/hole (e·Å ⁻³)	0.859 and -0.624	1.123 and -0.504	1.115 and -1.083	1.050 and -0.786
CCDC no.	1916223	1916225	1916224	1916226